

A numerical approximation method for the Fisher-Rao distance between multivariate normal distributions

Frank Nielsen

ORCID ID:0000-0001-5728-0726

Sony Computer Science Laboratories Inc, Tokyo, Japan.

Abstract

We present a simple method to approximate Rao's distance between multivariate normal distributions based on discretizing curves joining normal distributions and approximating Rao distances between successive nearby normal distributions on the curve by Jeffreys divergence. We consider experimentally the linear interpolation curves in the ordinary, natural and expectation parameterizations of the normal distributions, and compare these curves with a curve derived from the Calvo and Oller's isometric embedding of the Fisher-Rao d -variate normal manifold into the cone of $(d+1) \times (d+1)$ symmetric positive-definite matrices [Journal of multivariate analysis 35.2 (1990): 223-242]. We report on our experiments and assess the quality of our approximation technique by comparing the numerical approximations with lower and upper bounds. Finally, we present some information-geometric properties of the Calvo and Oller's isometric embedding.

Keywords: Fisher-Rao normal manifold; symmetric positive-definite matrix cone; isometric embedding; information geometry

1 Introduction

Let $\mathcal{P}(d)$ denote the set of symmetric positive-definite matrices (a convex regular cone), and $\mathcal{N}(d) = \{N(\mu, \Sigma) : (\mu, \Sigma) \in \mathbb{R}^d \times \mathcal{P}(d)\}$ denote the set of d -variate normal distributions (or Gaussians) with

$$N(\mu, \Sigma) \sim p_{\lambda=(\mu, \Sigma)}(x) = (2\pi)^{\frac{d}{2}} |\Sigma|^{-\frac{1}{2}} \exp\left(-\frac{1}{2}(x - \mu)^\top \Sigma^{-1}(x - \mu)\right), x \in \mathbb{R}^d.$$

The statistical model $\mathcal{N}(d)$ is of dimension $d + \frac{d(d+1)}{2} = \frac{d(d+3)}{2}$. By equipping $\mathcal{N}(d)$ with the Fisher information metric

$$g_{\mathcal{N}}^{\text{Fisher}}(\mu, \Sigma) = -E[\nabla^2 \log p_{(\mu, \Sigma)}(x)],$$

we get a Riemannian manifold called the Fisher-Rao Gaussian [30] with Riemannian geodesic distance $\rho_{\mathcal{N}}(\cdot, \cdot)$ called the Rao distance [3] or Fisher-Rao distance [28, 19, 8]. Historically, Hotelling [12] first used this distance in the late 1920's. The squared line element $ds_{\mathcal{N}}^2(\mu, \Sigma) = g_{(\mu, \Sigma)}^{\text{Fisher}}(d\mu, d\Sigma)$ induced by the Fisher information metric of the normal family is

$$ds_{\mathcal{N}}^2(\mu, \Sigma) = d\mu^\top \Sigma^{-1} d\mu + \frac{1}{2} \text{tr}\left((\Sigma^{-1} d\Sigma)^2\right).$$

In general, the Fisher-Rao distance between multivariate normal distributions is not known in closed-form [10, 13, 14], and several lower and upper bounds [31], and numerical techniques like geodesic shooting [11, 25, 4] have been investigated: See [26] for a review. The two difficulties to calculate the Fisher-Rao distance are (1) to know explicitly the expression of the Riemannian Fisher-Rao geodesic $\gamma_{\mathcal{N}}^{\text{FR}}$ and (2) to integrate in closed-form the length element $ds_{\mathcal{N}}$ along this Riemannian geodesic. However, in several special cases, the Fisher-Rao distance between normal distributions is known. Two such cases are when the normal distributions are univariate ($d = 1$) and when the normal distributions belong to some submanifold $\mathcal{N}_{\mu} = \{N(\mu, \Sigma) : \Sigma \in \mathcal{P}(d)\} \subset \mathcal{N}$ of normal distributions sharing the same mean μ . In the first case, the Fisher-Rao distance between $N_1 = N(\mu_1, \sigma_1^2)$ and $N_2 = N(\mu_2, \sigma_2^2)$ can be derived from the hyperbolic distance expressed in the Poincaré upper space:

$$\rho_{\mathcal{N}}(N_1, N_2) = \sqrt{2} \log \frac{1 + \Delta(\mu_1, \sigma_1; \mu_2, \sigma_2)}{1 - \Delta(\mu_1, \sigma_1; \mu_2, \sigma_2)},$$

with

$$\Delta(a, b; c, d) = \sqrt{\frac{(c - a)^2 + 2(d - b)^2}{(c - a)^2 + 2(d + b)^2}}.$$

In the second case, Rao distance between $N_1 = N(\mu, \Sigma_1)$ and $N_2 = N(\mu, \Sigma_2)$ has been reported in [15, 30] (see also [36]):

$$\rho_{\mathcal{N}}(N_1, N_2) = \sqrt{\frac{1}{2} \sum_{i=1}^d \log^2 \lambda_i(\Sigma_1^{-1} \Sigma_2)},$$

where $\lambda_i(M)$ denotes the i -th largest eigenvalue of matrix M . In general, the difficulty of calculating the Fisher-Rao distance comes from the fact that (1) we do not know the Fisher-Rao geodesics with boundary value conditions in closed form (only the geodesics with initial value conditions [7] are known), (2) we have to integrate the line element $ds_{\mathcal{N}}$ along the geodesic. The lack of closed-form formula and fast and good approximations for $\rho_{\mathcal{N}}$ between normals is a current limiting factor for applications. The geometry of zero-centered generalized multivariate Gaussians was recently studied in [34].

The main contribution of this paper is to propose an approximation of $\rho_{\mathcal{N}}$ based on Calvo & Oller's embedding [5] and report its experimental performance. First, we concisely recall Calvo and Oller's family of embeddings f_{β} of $\mathcal{N}(d)$ as submanifolds $\overline{\mathcal{N}}_{\beta}$ of $\mathcal{P}(d + 1)$ in Section 2. Next, we present our approximation technique in Section 3 which differs from the usual geodesic shooting approach [11], and report experimental results. Finally, we study some information-geometric properties [1] of the isometric embedding in §4 like the fact that it preserves mixture but not exponential geodesics.

2 Calvo and Oller's family of embeddings

Calvo and Oller [5, 6] noticed that we can embed normal distributions in $\mathcal{P}(d + 1)$ by the following mapping:

$$f_{\beta}(\mu, \Sigma) = \begin{bmatrix} \Sigma + \beta \mu \mu^{\top} & \beta \mu \\ \beta \mu^{\top} & \beta \end{bmatrix} \in \mathcal{P}(d + 1), \quad (1)$$

where $\beta \in \mathbb{R}_{>0}$. Notice that since the dimension of $\mathcal{P}(d+1)$ is $\frac{(d+1)(d+2)}{2}$, we only use $\frac{(d+1)(d+2)}{2} - \frac{d(d+3)}{2} = 1$ extra dimension for embedding $\mathcal{N}(d)$ into $\mathcal{P}(d+1)$. Let

$$\overline{\mathcal{N}}_\beta(d) = \left\{ \bar{P} = f_\beta(\mu, \Sigma) : (\mu, \Sigma) \in \mathbb{R}^d \times \mathcal{P}(d) \right\}$$

denote the submanifold of $\mathcal{P}(d+1)$ of codimension 1, and $\overline{\mathcal{N}} = \overline{\mathcal{N}}_1$. The family of mappings f_β provides diffeomorphisms between $\mathcal{N}(d)$ and $\overline{\mathcal{N}}_\beta(d)$. Let $f_\beta^{-1}(\bar{P}) = (\mu_{\bar{P}}, \Sigma_{\bar{P}})$ denote the inverse mapping, and let $f = f_1$.

By equipping the cone $\mathcal{P}(d+1)$ by the trace metric [18]

$$g_P^{\text{trace}}(P_1, P_2) = \text{tr}(P^{-1}P_1P^{-1}P_2)$$

scaled by $\frac{1}{2}$ (yielding the squared line element $ds_{\mathcal{P}}^2 = \frac{1}{2}\text{tr}((PdP)^2)$), Calvo and Oller [5] proved that $\overline{\mathcal{N}}(d)$ is isometric to $\mathcal{N}(d)$ (i.e., the Riemannian metric of $\mathcal{P}(d+1)$ restricted to $\overline{\mathcal{N}}(d)$ coincides with the Riemannian metric of $\mathcal{N}(d)$ induced by f) but $\overline{\mathcal{N}}(d)$ is not totally geodesic (i.e., the geodesics $\gamma_{\mathcal{P}}(\bar{P}_1, \bar{P}_2; t)$ for $\bar{P}_1 = f(N_1), \bar{P}_2 = f(N_2) \in \overline{\mathcal{N}}(d)$ leaves the embedded normal submanifold $\overline{\mathcal{N}}(d)$). Note that the trace metric was first studied by Siegel [29, 21] using the wider scope of complex symmetric matrices with positive-definite imaginary parts generalizing the Poincaré upper half-plane.

We omit to specify the dimensions and write for short \mathcal{N} , $\overline{\mathcal{N}}$ and \mathcal{P} when clear from context. Thus Calvo and Oller proposed to use the embedding $f = f_1$ to give a lower bound ρ_{CO} of the Fisher-Rao distance $\rho_{\mathcal{N}}$ between normals:

$$\rho_{\mathcal{N}}(N_1, N_2) \geq \rho_{\text{CO}}(\underbrace{f(\mu_1, \Sigma_1)}_{\bar{P}_1}, \underbrace{f(\mu_2, \Sigma_2)}_{\bar{P}_2}) = \sqrt{\frac{1}{2} \sum_{i=1}^{d+1} \log^2 \lambda_i(\bar{P}_1^{-1}\bar{P}_2)}.$$

The Calvo & Oller distance ρ_{CO} is a metric distance that has been used in many applications ranging from computer vision to signal/sensor processing and machine learning [32, 35, 16, 17, 24].

Remark 1 *In a second paper, Calvo and Oller [6] noticed that we can embed normal distributions in $\mathcal{P}(d+1)$ by the following mapping (Lemma 3.1 [6]):*

$$g_{\alpha, \beta, \gamma}(\mu, \Sigma) = |\Sigma|^\alpha \begin{bmatrix} \Sigma + \beta\gamma^2\mu\mu^\top & \beta\gamma\mu \\ \beta\gamma\mu^\top & \beta \end{bmatrix} \in \mathcal{P}(d+1),$$

where $\alpha \in \mathbb{R}$, $\beta \in \mathbb{R}_{>0}$ and $\gamma \in \mathbb{R}$. In some applications [27], the embedding $g_{-\frac{1}{d+1}, 1, 1}(\mu, \Sigma) = |\Sigma|^{-\frac{1}{d+1}} \begin{bmatrix} \Sigma + \mu\mu^\top & \mu \\ \mu^\top & 1 \end{bmatrix}$ is used to ensure that $|g_{-\frac{1}{d+1}, 1, 1}(\mu, \Sigma)| = 1$. That is normal distributions are embedded diffeomorphically into the submanifold of positive-definite matrices with unit determinant (also called SSPD, acronym of Special SPD).

3 Approximating the Fisher-Rao distance

3.1 Approximating length of curves on \mathcal{N}

Rao's distance is a Riemannian geodesic distance

$$\rho_{\mathcal{N}}(p_{\lambda_1}, p_{\lambda_2}) = \inf_c \{ \text{Length}(c) : c(0) = p_{\lambda_1}, c(1) = p_{\lambda_2} \},$$

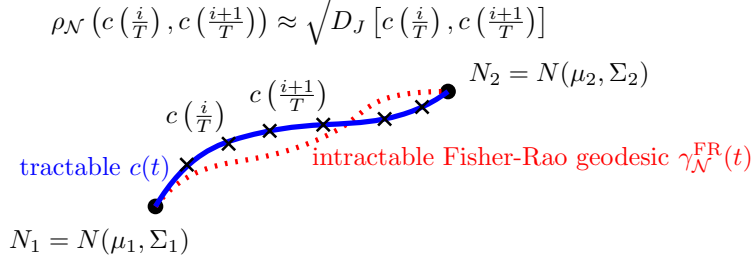


Figure 1: Approximating the Fisher-Rao geodesic distance $\rho_{\mathcal{N}}(N_1, N_2)$: The Fisher-Rao geodesic $\gamma_{\mathcal{N}}^{\text{FR}}$ is not known in closed-form. We consider a tractable curve $c(t)$, discretize $c(t)$ at $T + 1$ points $c(\frac{i}{T})$ with $c(0) = N_1$ and $c(1) = N_2$, and approximate $\rho_{\mathcal{N}}(c(\frac{i}{T}), c(\frac{i+1}{T}))$ by $D_J[c(\frac{i}{T}), c(\frac{i+1}{T})]$. Considering different tractable curves $c(t)$ yield different approximations.

where

$$\text{Length}(c) = \int_0^1 \underbrace{\sqrt{\langle \dot{c}(t), \dot{c}(t) \rangle_{c(t)}}}_{ds_{\mathcal{N}}(t)} dt.$$

Thus we can approximate the Rao distance $\rho_{\mathcal{N}}(N_1, N_2)$ by discretizing regularly any smooth curve $c(t)$ joining N_1 ($t = 0$) to N_2 ($t = 1$):

$$\rho_{\mathcal{N}}(N_1, N_2) \leq \frac{1}{T} \sum_{i=1}^{T-1} \rho_{\mathcal{N}}\left(c\left(\frac{i}{T}\right), c\left(\frac{i+1}{T}\right)\right),$$

with equality holding iff $c(t) = \gamma_{\mathcal{N}}(N_1, N_2; t)$ is the Riemannian geodesic induced by the Fisher information metric.

When T is sufficiently large, the normal distributions $c(\frac{i}{T})$ and $c(\frac{i+1}{T})$ are close to each other, and we can approximate $\rho_{\mathcal{N}}(c(\frac{i}{T}), c(\frac{i+1}{T}))$ by $\sqrt{D_J[c(\frac{i}{T}), c(\frac{i+1}{T})]}$, where $D_J[N_1, N_2] = D_{\text{KL}}[N_1, N_2] + D_{\text{KL}}[N_2, N_1]$ is Jeffreys divergence, and D_{KL} is the Kullback-Leibler divergence:

$$D_{\text{KL}}[p_{(\mu_1, \Sigma_1)} : p_{(\mu_2, \Sigma_2)}] = \frac{1}{2} \left(\text{tr}(\Sigma_2^{-1} \Sigma_1) + \Delta \mu^\top \Sigma_2^{-1} \Delta \mu - d + \log \frac{|\Sigma_2|}{|\Sigma_1|} \right).$$

Thus the costly determinant computations cancel each others in Jeffreys divergence (i.e., $\log \frac{|\Sigma_2|}{|\Sigma_1|} + \log \frac{|\Sigma_1|}{|\Sigma_2|} = 0$) and we have:

$$D_J[p_{(\mu_1, \Sigma_1)} : p_{(\mu_2, \Sigma_2)}] = \text{tr} \left(\frac{\Sigma_2^{-1} \Sigma_1 + \Sigma_1^{-1} \Sigma_2}{2} - I \right) + \Delta \mu^\top \frac{\Sigma_1^{-1} + \Sigma_2^{-1}}{2} \Delta \mu.$$

Figure 1 summarizes our method to approximate the Fisher-Rao geodesic distance.

In general, it holds that $I_f[p : q] \approx \frac{f''(1)}{2} ds_{\text{Fisher}}^2$ between infinitesimally close distributions p and q ($ds \approx \sqrt{\frac{2I_f[p:q]}{f''(1)}}$), where I_f denotes a f -divergence [1]. The Jeffreys divergence is a f -divergence obtained for $f_J(u) = -\log u + u \log u$ with $f_J''(1) = 2$.

Although the definite integral of the length element along the Fisher-Rao geodesic $\gamma_{\mathcal{N}}^{\text{FR}}$ is not known in closed form (i.e., Fisher-Rao distance), the integral of the squared length element along

the mixture geodesic $\gamma_{\mathcal{N}}^m$ and exponential geodesic $\gamma_{\mathcal{N}}^e$ coincide with Jeffreys divergence [1]:

$$D_J[p_{\lambda_1}, p_{\lambda_2}] = \int_0^1 ds_{\mathcal{N}}^2(\gamma_{\mathcal{N}}^m(p_{\lambda_1}, p_{\lambda_2}; t))dt = \int_0^1 ds_{\mathcal{N}}^2(\gamma_{\mathcal{N}}^e(p_{\lambda_1}, p_{\lambda_2}; t))dt.$$

It follows the following property:

Property 1 (Fisher-Rao upper bound) *The Fisher-Rao distance between normal distributions is upper bounded by the square root of the Jeffreys divergence: $\rho_{\mathcal{N}}(N_1, N_2) \leq \sqrt{D_J(N_1, N_2)}$.*

Proof: Consider the Cauchy-Schwarz inequality for positive functions $f(t)$ and $g(t)$: $\int_0^1 f(t)g(t)dt \leq \sqrt{(\int_0^1 f(t)^2 dt)(\int_0^1 g(t)^2 dt)}$, and let $f(t) = ds_{\mathcal{N}}(\gamma_{\mathcal{N}}^c(p_{\lambda_1}, p_{\lambda_2}; t))$ and $g(t) = 1$. Then we get:

$$\left(\int_0^1 ds_{\mathcal{N}}(\gamma_{\mathcal{N}}^c(p_{\lambda_1}, p_{\lambda_2}; t))dt \right)^2 \leq \left(\int_0^1 ds_{\mathcal{N}}^2(\gamma_{\mathcal{N}}^c(p_{\lambda_1}, p_{\lambda_2}; t))dt \right) \left(\int_0^1 1^2 dt \right)$$

Furthermore since by definition of $\gamma_{\mathcal{N}}^{\text{FR}}$, we have $\int_0^1 ds_{\mathcal{N}}(\gamma_{\mathcal{N}}^c(p_{\lambda_1}, p_{\lambda_2}; t))dt \geq \int_0^1 ds_{\mathcal{N}}(\gamma_{\mathcal{N}}^{\text{FR}}(p_{\lambda_1}, p_{\lambda_2}; t))dt =: \rho_{\mathcal{N}}(N_1, N_2)$, it follows for $c = e$ (i.e., e -geodesic $\gamma_{\mathcal{N}}^e$), we have:

$$\rho_{\mathcal{N}}(N_1, N_2)^2 \leq \int_0^1 ds_{\mathcal{N}}^2(\gamma_{\mathcal{N}}^e(p_{\lambda_1}, p_{\lambda_2}; t))dt = D_J(N_1, N_2).$$

Thus we have $\rho_{\mathcal{N}}(N_1, N_2) \leq \sqrt{D_J(N_1, N_2)}$. □

For any smooth curve $c(t)$, we thus approximate $\rho_{\mathcal{N}}$ by

$$\boxed{\tilde{\rho}_{\mathcal{N}}(N_1, N_2) := \frac{1}{T} \sum_{i=1}^{T-1} \sqrt{D_J \left[c \left(\frac{i}{T} \right), c \left(\frac{i+1}{T} \right) \right]}.} \quad (2)$$

For example, we may consider the following curves on \mathcal{N} which admit closed-form parameterizations in $t \in [0, 1]$:

- linear interpolation $c_{\lambda}(t) = t(\mu_1, \Sigma_1) + (1-t)(\mu_2, \Sigma_2)$ between (μ_1, Σ_1) and (μ_2, Σ_2) ,
- the mixture geodesic [20] $c_m(t) = \gamma_{\mathcal{N}}^m(N_1, N_2; t) = (\mu_t^m, \Sigma_t^m)$ with $\mu_t^m = \bar{\mu}_t$ and $\Sigma_t^m = \bar{\Sigma}_t + t\mu_1\mu_1^{\top} + (1-t)\mu_2\mu_2^{\top} - \bar{\mu}_t\bar{\mu}_t^{\top}$ where $\bar{\mu}_t = t\mu_1 + (1-t)\mu_2$ and $\bar{\Sigma}_t = t\Sigma_1 + (1-t)\Sigma_2$,
- the exponential geodesic [20] $c_e(t) = \gamma_{\mathcal{N}}^e(N_1, N_2; t) = (\mu_t^e, \Sigma_t^e)$ with $\mu_t^e = \bar{\Sigma}_t^H(t\Sigma_1^{-1}\mu_1 + (1-t)\Sigma_2^{-1}\mu_2)$ and $\Sigma_t^e = \bar{\Sigma}_t^H$ where $\bar{\Sigma}_t^H = (t\Sigma_1^{-1} + (1-t)\Sigma_2^{-1})^{-1}$ is the matrix harmonic mean,
- the curve $c_{em}(t) = \frac{1}{2}(\gamma_{\mathcal{N}}^e(N_1, N_2; t) + \gamma_{\mathcal{N}}^m(N_1, N_2; t))$ which is obtained by averaging the mixture geodesic with the exponential geodesic.

Let us denote by $\tilde{\rho}_{\mathcal{N}}^{\lambda} = \tilde{\rho}_{\mathcal{N}}^{c_{\lambda}}$, $\tilde{\rho}_{\mathcal{N}}^m = \tilde{\rho}_{\mathcal{N}}^{c_m}$, $\tilde{\rho}_{\mathcal{N}}^e = \tilde{\rho}_{\mathcal{N}}^{c_e}$ and $\tilde{\rho}_{\mathcal{N}}^{em} = \tilde{\rho}_{\mathcal{N}}^{c_{em}}$ the approximations obtained by these curves following from Eq. 2.

Next, we introduce yet another curve $c_{\text{CO}}(t)$ derived from Calvo & Oller isometric mapping f which experimentally behaves better when normals are not too far from each others.

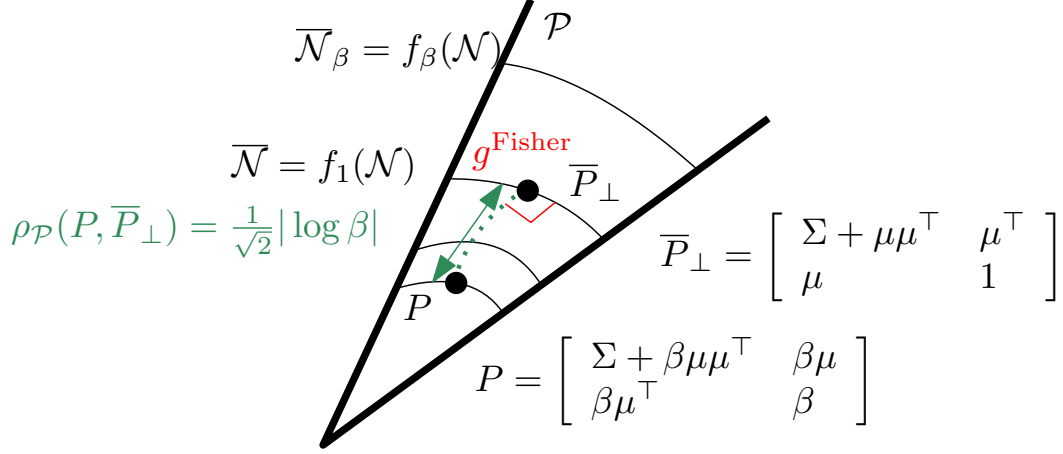


Figure 2: Projecting a SPD matrix $P \in \mathcal{P}$ onto $\bar{\mathcal{N}} = f(\mathcal{N})$.

3.2 Calvo & Oller's curve

This approximation consists in leveraging the closed-form expression of the SPD geodesics [18, 2]:

$$\gamma_{\mathcal{P}}(P, Q; t) = P^{\frac{1}{2}} \left(P^{-\frac{1}{2}} Q^{\frac{1}{2}} P^{-\frac{1}{2}} \right)^t P^{\frac{1}{2}},$$

to approximate the Fisher-Rao normal geodesic $\gamma_{\mathcal{N}}(N_1, N_2; t)$ as follows: Let $\bar{P}_1 = f(N_1)$, $\bar{P}_2 = f(N_2) \in \bar{\mathcal{N}}$, and consider the smooth curve

$$\bar{c}_{\text{CO}}(P_1, P_2; t) = \text{proj}_{\bar{\mathcal{N}}}(\gamma_{\mathcal{P}}(\bar{P}_1, \bar{P}_2; t)),$$

where $\text{proj}_{\bar{\mathcal{N}}}(P)$ denotes the Fisher orthogonal projection of $P \in \mathcal{P}(d+1)$ onto $\bar{\mathcal{N}}$ (Figure 3). Thus curve c_{CO} is then defined as $f^{-1}(\bar{c}_{\text{CO}})$. Note that the power matrix P^t is $U \text{diag}(\lambda_1^t, \dots, \lambda_d^t) V^{\top}$ where $P = U \text{diag}(\lambda_1^t, \dots, \lambda_d^t) V^{\top}$ is the eigenvalue decomposition of P .

Let us now explain how to project $P = [P_{i,j}] \in \mathcal{P}(d+1)$ onto $\bar{\mathcal{N}}$ based on the analysis of the Appendix of [5] (page 239):

Proposition 1 (Projection of a SPD matrix onto the embedded normal submanifold $\bar{\mathcal{N}}$)

Let $\beta = P_{d+1,d+1}$ and write $P = \begin{bmatrix} \Sigma + \beta \mu \mu^{\top} & \beta \mu \\ \beta \mu^{\top} & \beta \end{bmatrix}$. Then the orthogonal projection at $P \in \mathcal{P}$ onto $\bar{\mathcal{N}}$ is:

$$\bar{P}_{\perp} = \text{proj}_{\bar{\mathcal{N}}}(P) = \begin{bmatrix} \Sigma + \mu \mu^{\top} & \mu^{\top} \\ \mu & 1 \end{bmatrix},$$

and the SPD distance between P and \bar{P}_{\perp} is $\rho_{\mathcal{P}}(P, \bar{P}_{\perp}) = \frac{1}{\sqrt{2}} |\log \beta|$.

Note that the introduction of parameter β is related to the foliation of the SPD cone \mathcal{P} by $\{f_{\beta}(\mathcal{N}) : \beta > 0\}$: $\mathcal{P}(d+1) = \mathbb{R}_{>0} \times f_{\beta}(\mathcal{N})$. See Figure 2.

Let $\bar{c}_{\text{CO}}(t) = \bar{S}_t$ and $c_{\text{CO}}(t) = f^{-1}(\bar{c}_{\text{CO}}(t)) =: G_t$. The following proposition shows that we have $D_J[\bar{S}_t, \bar{S}_{t+1}] = D_J[G_t, G_{t+1}]$.

Proposition 2 The Kullback-Leibler divergence between p_{μ_1, Σ_1} and p_{μ_2, Σ_2} amounts to the KLD between $q_{\bar{P}_1} = p_{0, f(\mu_1, \Sigma_1)}$ and $q_{\bar{P}_2} = p_{0, f(\mu_2, \Sigma_2)}$ where $\bar{P}_i = f(\mu_i, \Sigma_i)$:

$$D_{\text{KL}}[p_{\mu_1, \Sigma_1} : p_{\mu_2, \Sigma_2}] = D_{\text{KL}}[q_{\bar{P}_1} : q_{\bar{P}_2}].$$

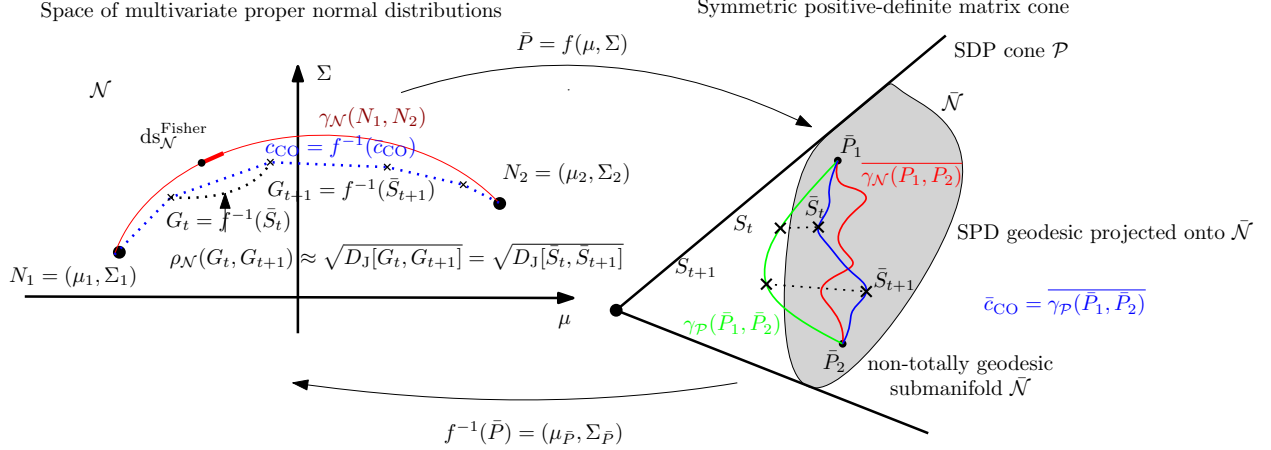


Figure 3: Illustration of the approximation of the Fisher-Rao distance between two normals N_1 and N_2 (red geodesic length $\gamma_{\mathcal{N}}(N_1, N_2)$) by discretizing $\bar{c}_{\text{CO}} \in \bar{\mathcal{N}}$ or equivalently $c_{\text{CO}} \in \mathcal{N}$.

Proof: The KLD between two centered $(d+1)$ -variate normals $q_{P_1} = p_{0, P_1}$ and $q_{P_2} = p_{0, P_2}$ is

$$D_{\text{KL}}[q_{P_1} : q_{P_2}] = \frac{1}{2} \left(\text{tr}(P_2^{-1} P_1) - d - 1 + \log \frac{|P_2|}{|P_1|} \right).$$

This divergence can be interpreted as the matrix version of the Itakura-Saito divergence [9]. The SPD cone equipped with $\frac{1}{2}$ of the trace metric can be interpreted as Fisher-Rao centered normal manifolds: $(\mathcal{N}_\mu, g_{\mathcal{N}_\mu}^{\text{Fisher}}) = (\mathcal{P}, \frac{1}{2} g^{\text{trace}})$.

Since the determinant of a block matrix is

$$\left| \begin{bmatrix} A & B \\ C & D \end{bmatrix} \right| = |A - BD^{-1}C|,$$

we get with $D = 1$: $|f(\mu, \Sigma)| = |\Sigma + \mu\mu^\top - \mu\mu^\top| = |\Sigma|$.

Let $\bar{P}_1 = f(\mu_1, \Sigma_1)$ and $\bar{P}_2 = f(\mu_2, \Sigma_2)$. Checking $D_{\text{KL}}[p_{\mu_1, \Sigma_1} : p_{\mu_2, \Sigma_2}] = D_{\text{KL}}[q_{\bar{P}_1} : q_{\bar{P}_2}]$ where $q_{\bar{P}} = p_{0, \bar{P}}$ amounts to verify that

$$\text{tr}(\bar{P}_2^{-1} \bar{P}_1) = 1 + \text{tr}(\Sigma_2^{-1} \Sigma_1 + \Delta_\mu^\top \Sigma_2^{-1} \Delta_\mu).$$

Indeed, using the inverse matrix

$$f(\mu, \Sigma)^{-1} = \begin{bmatrix} \Sigma^{-1} & -\Sigma^{-1}\mu \\ -\mu^\top \Sigma^{-1} & 1 + \mu^\top \Sigma^{-1} \mu \end{bmatrix},$$

we have $\text{tr}(\bar{P}_2^{-1} \bar{P}_1) = \text{tr} \left(\begin{bmatrix} \Sigma_2^{-1} & -\Sigma_2^{-1} \mu_2 \\ -\mu_2^\top \Sigma_2^{-1} & 1 + \mu_2^\top \Sigma_2^{-1} \mu_2 \end{bmatrix} \begin{bmatrix} \Sigma_1 + \mu_1 \mu_1^\top & \mu_1 \\ \mu_1^\top & 1 \end{bmatrix} \right) = 1 + \text{tr}(\Sigma_2^{-1} \Sigma_1 + \Delta_\mu^\top \Sigma_2^{-1} \Delta_\mu)$. Thus even if the dimension of the sample spaces of $p_{\mu, \Sigma}$ and $q_{\bar{P}=f(\mu, \Sigma)}$ differs by one, we get the same KLD by Calvo and Oller's isometric mapping f . \square

This property holds for the KLD/Jeffreys divergence but not for all f -divergences [1] I_f in general (e.g., it fails for the Hellinger divergence).

Table 1: First set of experiments demonstrates the advantage of the $c_{\text{CO}}(t)$ curve.

d	κ_{CO}	κ_l	κ_e	κ_m	κ_{em}
1	1.0025	1.0414	1.1521	1.0236	1.0154
2	1.0167	1.0841	1.1923	1.0631	1.0416
3	1.0182	1.8997	2.6072	1.9965	1.07988
4	1.0207	2.0793	1.8080	2.1687	1.1873
5	1.0324	4.1207	12.3804	5.6170	4.2349

3.3 Some experiments

The KLD D_{KL} and Jeffreys divergence D_J , the Fisher-Rao distance $\rho_{\mathcal{N}}$ and the Calvo & Oller distance ρ_{CO} are all invariant under the congruence action of the affine group $\text{Aff}(d) = \mathbb{R}^d \rtimes \text{GL}(d)$ with group operation

$$(a_1, A_1)(a_2, A_2) = (a_1 + A_1 a_2, A_1 A_2).$$

Let $(A, a) \in \text{Aff}(d)$, and define the action on the normal space \mathcal{N} as follows:

$$(A, a).N(\mu, \Sigma) = N(A^\top \mu + a, A \Sigma A^\top).$$

Then we have $\rho_{\mathcal{N}}((A, a).N_1, (A, a).N_2) = \rho_{\mathcal{N}}(N_1, N_2)$, $\rho_{\text{CO}}((A, a).N_1, (A, a).N_2) = \rho_{\text{CO}}(N_1, N_2)$ and $D_{\text{KL}}[(A, a).N_1 : (A, a).N_2] = D_{\text{KL}}[N_1 : N_2]$. This invariance extends to our approximations $\tilde{\rho}_{\mathcal{N}}^c$ (see Eq. 2).

Since we have

$$\tilde{\rho}_{\mathcal{N}}^c(N_1, N_2) \approx \rho_{\mathcal{N}}(N_1, N_2) \geq \rho_{\text{CO}}(N_1, N_2),$$

the ratio $\kappa_c = \frac{\tilde{\rho}_{\mathcal{N}}^c}{\rho_{\text{CO}}} \geq \kappa = \frac{\tilde{\rho}_{\mathcal{N}}^c}{\rho_{\mathcal{N}}}$ gives an upper bound on the approximation factor of $\tilde{\rho}_{\mathcal{N}}^c$ compared to the true Fisher-Rao distance $\rho_{\mathcal{N}}$:

$$\kappa_c \rho_{\mathcal{N}}(N_1, N_2) \geq \kappa \rho_{\mathcal{N}}(N_1, N_2) \geq \tilde{\rho}_{\mathcal{N}}^c(N_1, N_2) \approx \rho_{\mathcal{N}}(N_1, N_2) \geq \rho_{\text{CO}}(N_1, N_2).$$

Let us now report some numerical experiments of our approximated Fisher-Rao distances $\tilde{\rho}_{\mathcal{N}}^x$ with $x \in \{l, m, e, em, \text{CO}\}$. Although that dissimilarity $\tilde{\rho}_{\mathcal{N}}$ is positive-definite, it does not satisfy the triangular inequality of metric distances (e.g., Riemannian distances $\rho_{\mathcal{N}}$ and ρ_{CO}).

First, we draw multivariate normals by sampling means $\mu \sim \text{Unif}(0, 1)$ and sample covariance matrices Σ as follows: We draw a lower triangular matrix L with entries L_{ij} iid sampled from $\text{Unif}(0, 1)$, and take $\Sigma = LL^\top$. We use $T = 1000$ samples on curves and repeat the experiment 1000 times to gather average statistics on κ_c 's of curves. Results are summarized in Table 1.

For that scenario that the C&O curve (either $\bar{c}_{\text{CO}} \in \bar{\mathcal{N}}$ or $c_{\text{CO}} \in \mathcal{N}$) performs best compared to the linear interpolation curves with respect to source parameter (l), mixture geodesic (m), exponential geodesic (e), or exponential-mixture mid curve (em). Let us point out that we sample $\gamma_{\mathcal{P}}(\bar{P}_1, \bar{P}_2; \frac{i}{T})$ for $i \in \{0, \dots, T\}$.

Strapasson et al. [31] reported the following upper bound on the Fisher-Rao distance between multivariate normals:

$$\rho_{\text{CO}}(N_1, N_2) \leq \rho_{\mathcal{N}}(N_1, N_2) \leq U(N_1, N_2) = \sqrt{2 \sum_{i=1}^d \log^2 \left(\frac{\sqrt{(1 + D_{ii})^2 + \mu_i^2} + \sqrt{(1 - D_{ii})^2 + \mu_i^2}}{\sqrt{(1 + D_{ii})^2 + \mu_i^2} - \sqrt{(1 - D_{ii})^2 + \mu_i^2}} \right)}, \quad (3)$$

Table 2: Comparing our Fisher-Rao approximation with the Calvo & Oller lower bound and the Strapasson et al. upper bound.

d	$\rho_{\text{CO}}(N_1, N_2)$	$\tilde{\rho}^{\text{cco}}(N_1, N_2)$	$U(N_1, N_2)$
1	1.7563	1.8020	3.1654
2	3.2213	3.3194	6.012
3	4.6022	4.7642	8.7204
4	5.9517	6.1927	11.3990
5	7.156	7.3866	13.8774



Figure 4: Visualizing some Fisher-Rao geodesics of univariate normal distributions on the Poincaré upper plane (semi-circles with origin on the x -axis and stretched by $\sqrt{2}$ on the x -axis). Full geodesics plotted with thin style and geodesic arcs plotted with thick style.

where $\Sigma = \Sigma_1^{-\frac{1}{2}} \Sigma_2 \Sigma_1^{-\frac{1}{2}}$, $\Sigma = \Omega D \Omega^\top$ is the eigen decomposition, and $\mu = \Omega^\top \Sigma_1^{-\frac{1}{2}} (\mu_2 - \mu_1)$.

Let us compare $\rho_{\text{CO}}(N_1, N_2)$ with $\rho_{\mathcal{N}}(N_1, N_2) \approx \tilde{\rho}^{\text{cco}}(N_1, N_2)$ and the upper bound $U(N_1, N_2)$ by averaging over 1000 trials with N_1 and N_2 chosen randomly as before and $T = 1000$. We have $\rho_{\text{CO}}(N_1, N_2) \leq \rho_{\mathcal{N}}(N_1, N_2) \approx \tilde{\rho}^{\text{cco}}(N_1, N_2) \leq U(N_1, N_2)$. Table 2 shows that our Fisher-Rao approximation is close to the lower bound (and hence to the underlying true Fisher-Rao distance) and that the upper bound is about twice the lower bound for that particular scenario. Notice that the upper bound $\rho_{\mathcal{N}}(N_1, N_2) \leq \sqrt{D_J(N_1, N_2)}$ of Proposition 1 behaves experimentally much looser than the upper bound of Strapasson et al. [31].

The Fisher-Rao geodesics $\gamma_{\mathcal{N}}^{\text{FR}}(N_1, N_2)$ on the Fisher-Rao univariate normal manifolds are either vertical line segments when $\mu_1 = \mu_2$, or semi-circle with origin on the x -axis and x -axis stretched by $\sqrt{2}$ [33]:

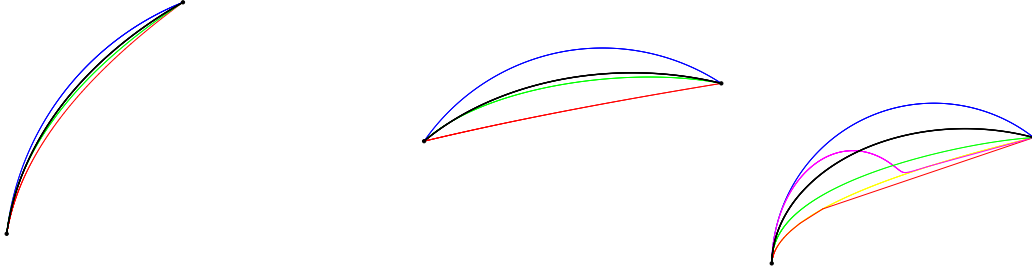


Figure 5: Visualizing the geodesics and curves in the Poincaré upper plane with x -axis stretched by $\sqrt{2}$: (a) and (b): Fisher-Rao geodesic (black), our projected Calvo & Oller curve (green), the mixture geodesic (blue), and the exponential geodesic (red). (c): interpolation in ordinary parameterization λ (yellow), mid mixture-exponential curve (purple). The range is $[-1, 1] \times (0, 2]$.

$$\gamma_{\mathcal{N}}^{\text{FR}}(\mu_1, \sigma_1; \mu_2, \sigma_2) = \begin{cases} (\mu, (1-t)\sigma_1 + t\sigma_2), & \mu_1 = \mu_2 = \mu \\ (\sqrt{2}(c + r \cos t), r \sin t), t \in [\min\{\theta_1, \theta_2\}, \max\{\theta_1, \theta_2\}], & \mu_1 \neq \mu_2, \end{cases},$$

where

$$c = \frac{\frac{1}{2}(\mu_2^2 - \mu_1^2) + \sigma_2^2 - \sigma_1^2}{\sqrt{2}(\mu_1 - \mu_2)}, \quad r = \sqrt{\left(\frac{\mu_i}{\sqrt{2}} - c\right)^2 + \sigma_i^2}, i \in \{1, 2\},$$

and

$$\theta_i = \arctan\left(\frac{\sigma_i}{\frac{\mu_i}{\sqrt{2}} - c}\right), i \in \{1, 2\},$$

provided that $\theta_i \geq 0$ for $i \in \{1, 2\}$ (otherwise, we let $\theta_i \leftarrow \theta_i + \pi$). Figure 4 displays some geodesics on the Fisher-Rao univariate normal manifold. Figure 5 displays the considered geodesics and curves in the stretched Poincaré upper plane of univariate normal distributions (x -axis is stretched by $\sqrt{2}$) (in 1D for illustration purpose).

Second, since the distances are invariant under the action of the affine group, we can set wlog. $N_1 = (0, I)$ (standard normal distribution) and let $N_2 = \text{diag}(u_1, \dots, u_d)$ where $u_i \sim \text{Unif}(0, a)$. As normals N_1 and N_2 separate to each others, we notice experimentally that the performance of the c_{CO} curve degrades in the second experiment with $a = 5$ (see Table 3): Indeed, the mixture geodesic works experimentally better than the C&O curve when $d \geq 11$.

Figure 6 and Figure 7 display the various curves considered for approximating the Fisher-Rao distance between bivariate normal distributions: For a curve $c(t)$, we visualize its corresponding bivariate normal distributions $(\mu_{c(t)}, \Sigma_{c(t)})$ at several increment steps $t \in [0, 1]$ by plotting the ellipsoid

$$E_{c(t)} = \mu_{c(t)} + \left\{ L^\top x, x = (\cos \theta, \sin \theta), \theta \in [0, 2\pi) \right\},$$

where $\Sigma_{c(t)} = L_{c(t)} L_{c(t)}^\top$.

Table 3: Second set of experiments shows limitations of the $c_{\text{CO}}(t)$ curve.

d	κ_{CO}	κ_l	κ_e	κ_m
1	1.0569	1.1405	1.139	1.0734
5	1.1599	1.4696	1.5201	1.1819
10	1.2180	1.6963	1.7887	1.2184
11	1.2260	1.7333	1.8285	1.2235
12	1.2301	1.7568	1.8539	1.2282
15	1.2484	1.8403	1.9557	1.2367
20	1.2707	1.9519	2.0851	1.2466

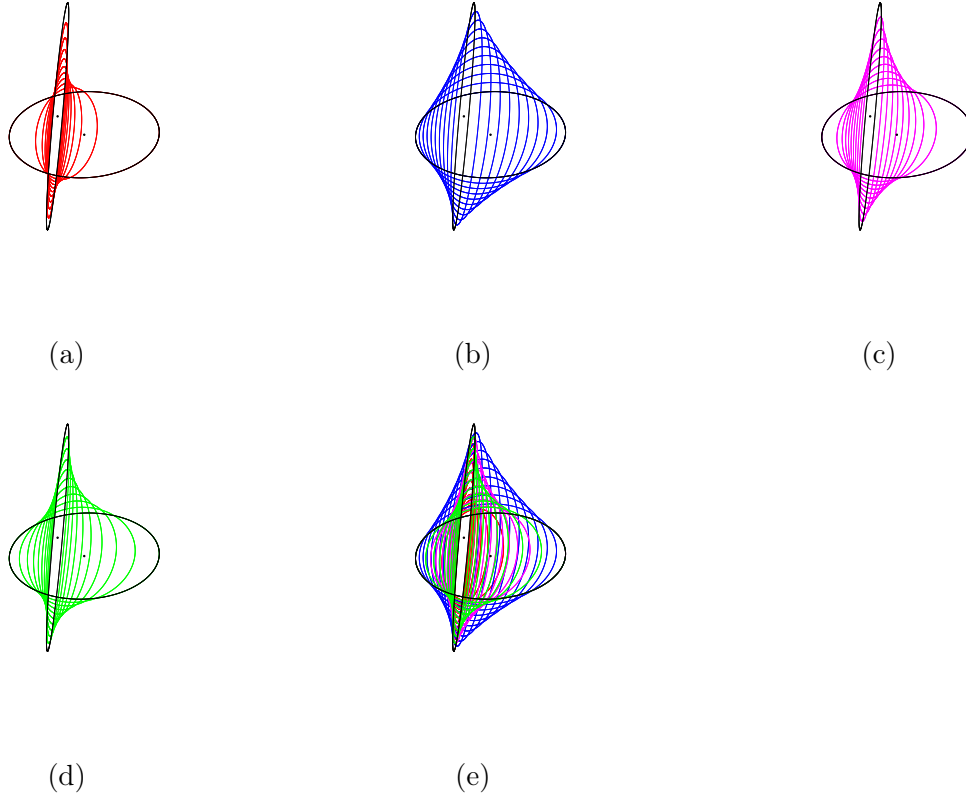


Figure 6: Visualizing at discrete positions (10 increment steps between 0 and 1) some curves used to approximate the Fisher-Rao distance between two bivariate normal distributions: (a) exponential geodesic $c^e = \gamma_{\mathcal{N}}^e$ (red), (b) mixture geodesic $c^m = \gamma_{\mathcal{N}}^m$ (blue), (c) mid mixture-exponential curve c^{em} (purple), (d) projected Calvo & Oller curve c^{CO} (green), and (e) All superposed curves at once.

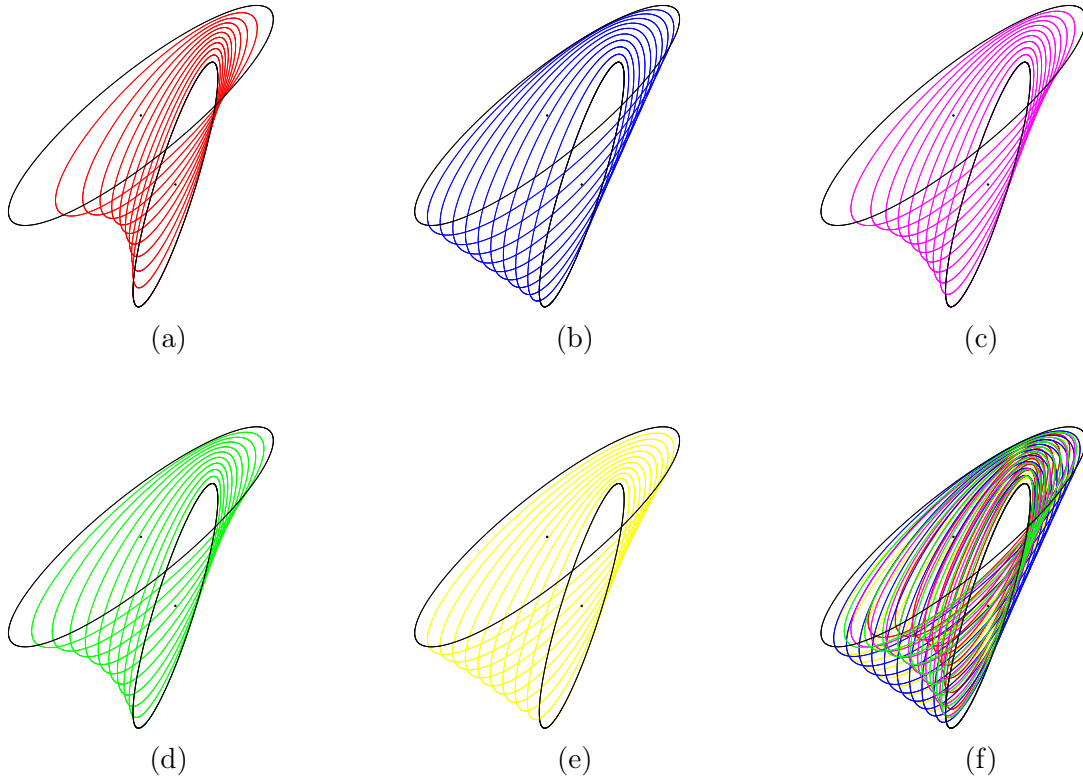


Figure 7: Visualizing at discrete positions (10 increment steps between 0 and 1) some curves used to approximate the Fisher-Rao distance between two bivariate normal distributions: (a) exponential geodesic $c^e = \gamma_{\mathcal{N}}^e$ (red), (b) mixture geodesic $c^m = \gamma_{\mathcal{N}}^m$ (blue), (c) mid mixture-exponential curve c^{em} (purple), (d) projected Calvo & Oller curve c^{CO} (green), (e) c^λ : ordinary linear interpolation in λ (yellow), and (f) All superposed curves at once.

4 Information-geometric properties of the embedding

In information geometry [1], the manifold \mathcal{N} admits a dual structure $(\mathcal{N}, g_{\mathcal{N}}^{\text{Fisher}}, \nabla_{\mathcal{N}}^e, \nabla_{\mathcal{N}}^m)$ when equipped with the exponential connection $\nabla_{\mathcal{N}}^e$ and the mixture connection $\nabla_{\mathcal{N}}^m$. The connections $\nabla_{\mathcal{N}}^e$ and $\nabla_{\mathcal{N}}^m$ are said dual since $\frac{\nabla_{\mathcal{N}}^e + \nabla_{\mathcal{N}}^m}{2} = \bar{\nabla}_{\mathcal{N}}$, the Levi-Civita connection induced by $g_{\mathcal{N}}^{\text{Fisher}}$. Furthermore, by viewing \mathcal{N} as an exponential family $\{p_{\theta}\}$ with natural parameter $\theta = (\theta_v, \theta_M)$ (using the sufficient statistics [20] $(x, -xx^{\top})$), and taking the convex log-normalizer function $F_{\mathcal{N}}(\theta)$ of the normals, we can build a dually flat space [1] where the canonical divergence amounts to a Bregman divergence which coincides with the reverse Kullback-Leibler divergence (KLD). The Legendre duality

$$F^*(\eta) = \langle \nabla F(\theta), \eta \rangle - F(\nabla F(\theta))$$

(with $\langle (v_1, M_1), (v_2, M_2) \rangle = v_1^{\top} v_2 + \text{tr}(M_1 M_2)$) yields: $\theta = (\theta_v, \theta_M) = (\Sigma^{-1} \mu, \frac{1}{2} \Sigma^{-1})$,

$$F_{\mathcal{N}}(\theta) = \frac{1}{2} \left(d \log \pi - \log |\theta_M| + \frac{1}{2} \theta_v^{\top} \theta_M^{-1} \theta_v \right),$$

$$\eta = (\eta_v, \eta_M) = \nabla F_{\mathcal{N}}(\theta) = \left(\frac{1}{2} \theta_M^{-1} \theta_v, \theta_M^{-1} \right),$$

$$F_{\mathcal{N}}^*(\eta) = -\frac{1}{2} \left(\log(1 + \eta_v^{\top} \eta_M^{-1} \eta_v) + \log |-\eta_M| + d(\log 2\pi e) \right),$$

and we have

$$B_{F_{\mathcal{N}}}(\theta_1, \theta_2) = D_{\text{KL}}^*(p_{\lambda_1} : p_{\lambda_2}) = D_{\text{KL}}(p_{\lambda_2} : p_{\lambda_1}) = B_{F_{\mathcal{N}}^*}(\eta_2 : \eta_1),$$

where $D_{\text{KL}}^*[p : q] = D_{\text{KL}}[q : p]$ is the reverse KLD.

In a dually flat space, we can express the canonical divergence as a Fenchel-Young divergence using the mixed coordinate systems $B_{F_{\mathcal{N}}}(\theta_1 : \theta_2) = Y_{F_{\mathcal{N}}}(\theta_1 : \eta_2)$ where $\eta_i = \nabla F_{\mathcal{N}}(\theta_i)$ and

$$Y_{F_{\mathcal{N}}}(\theta_1 : \eta_2) := F_{\mathcal{N}}(\theta_1) + F_{\mathcal{N}}^*(\eta_2) - \langle \theta_1, \eta_2 \rangle.$$

The moment η -parameterization of a normal is $(\eta = \mu, H = -\Sigma - \mu\mu^{\top})$ with its reciprocal function $(\lambda = \eta, \Lambda = -H - \eta\eta^{\top})$.

Let $F_{\mathcal{P}}(P) = F_{\mathcal{N}}(0, P)$, $\bar{\theta} = \frac{1}{2} \bar{P}^{-1}$, $\bar{\eta} = \nabla F_{\mathcal{P}}(\bar{\theta})$. Then we have the following proposition which proves that the Fenchel-Young divergences in \mathcal{N} and $\bar{\mathcal{N}}$ (as a submanifold of \mathcal{P}) coincide:

Proposition 3 *We have*

$$\begin{aligned} D_{\text{KL}}[p_{\mu_1, \Sigma_1} : p_{\mu_2, \Sigma_2}] &= B_{F_{\mathcal{N}}}(\theta_2 : \theta_1) = Y_{F_{\mathcal{N}}}(\theta_2 : \eta_1) = Y_{F_{\mathcal{P}}}(\bar{\theta}_2 : \bar{\eta}_1) \\ &= B_{F_{\mathcal{P}}}(\bar{\theta}_2 : \bar{\theta}_1) = D_{\text{KL}}[p_{0, \bar{P}_1=f(\mu_1, \Sigma_2)} : p_{0, \bar{P}_2=f(\mu_2, \Sigma_2)}]. \end{aligned}$$

Consider now the ∇^e -geodesics and ∇^m -geodesics on \mathcal{N} (linear interpolation with respect to natural and dual moment parameterizations, respectively): $\gamma_{\mathcal{N}}^e(N_1, N_2; t) = (\mu_t^e, \Sigma_t^e)$ and $\gamma_{\mathcal{N}}^m(N_1, N_2; t) = (\mu_t^m, \Sigma_t^m)$.

Proposition 4 *The mixture geodesics are preserved by the embedding f : $f(\gamma_{\mathcal{N}}^m(N_1, N_2; t)) = \gamma_{\mathcal{P}}^m(f(N_1), f(N_2); t)$. The exponential geodesics are preserved for subspace of \mathcal{N} with fixed mean μ : \mathcal{N}_{μ} .*

Proof: For the m -geodesics, let us check that

$$f(\mu_t^m, \Sigma_t^m) = \begin{bmatrix} \Sigma_t^m + \mu_t \mu_t^{m\top} & \mu_t^m \\ \mu_t^m & 1 \end{bmatrix} = t \underbrace{f(\mu_1, \Sigma_1)}_{\bar{P}_1} + (1-t) \underbrace{f(\mu_2, \Sigma_2)}_{\bar{P}_2},$$

since $\Sigma_t^m + \mu_t \mu_t^{m\top} = \bar{\Sigma}_t + t\mu_1 \mu_1^\top + (1-t)\mu_2 \mu_2^\top = t(\Sigma_1 + \mu_1 \mu_1^\top) + (1-t)(\Sigma_2 + \mu_2 \mu_2^\top)$. Thus we have $f(\gamma_{\mathcal{N}}^m(N_1, N_2; t)) = \gamma_{\mathcal{P}}^m(\bar{P}_1, \bar{P}_2; t)$. \square

Therefore all algorithms on \mathcal{N} which only require m -geodesics or m -projections [1] by minimizing the right-hand side of the KLD can be implemented by algorithms on \mathcal{P} . See for example, the minimum enclosing ball approximation algorithm called BBC in [22]. Notice that $\bar{\mathcal{N}}_\mu$ (fixed mean normal submanifolds) preserve both mixture and exponential geodesics: The submanifolds $\bar{\mathcal{N}}_\mu$ are said doubly auto-parallel [23].

Acknowledgments. I warmly thank Frédéric Barbaresco (Thales) and Mohammad Emtiyaz Khan (Riken AIP) for fruitful discussions about this work.

References

- [1] Shun-ichi Amari. *Information Geometry and Its Applications*. Applied Mathematical Sciences. Springer Japan, 2016.
- [2] Marc Arnaudon and Frank Nielsen. On approximating the Riemannian 1-center. *Computational Geometry*, 46(1):93–104, 2013.
- [3] Colin Atkinson and Ann FS Mitchell. Rao’s distance measure. *Sankhyā: The Indian Journal of Statistics, Series A*, pages 345–365, 1981.
- [4] Frédéric Barbaresco. Souriau exponential map algorithm for machine learning on matrix Lie groups. In *Geometric Science of Information: 4th International Conference, GSI 2019, Toulouse, France, August 27–29, 2019, Proceedings 4*, pages 85–95. Springer, 2019.
- [5] Miquel Calvo and Josep M Oller. A distance between multivariate normal distributions based in an embedding into the Siegel group. *Journal of multivariate analysis*, 35(2):223–242, 1990.
- [6] Miquel Calvo and Josep M Oller. A distance between elliptical distributions based in an embedding into the Siegel group. *Journal of Computational and Applied Mathematics*, 145(2):319–334, 2002.
- [7] Miquel Calvo and Josep Maria Oller. An explicit solution of information geodesic equations for the multivariate normal model. *Statistics & Risk Modeling*, 9(1-2):119–138, 1991.
- [8] Xiangbing Chen, Jie Zhou, and Sanfeng Hu. Upper bounds for Rao distance on the manifold of multivariate elliptical distributions. *Automatica*, 129:109604, 2021.
- [9] Jason Davis and Inderjit Dhillon. Differential entropic clustering of multivariate Gaussians. *Advances in Neural Information Processing Systems*, 19, 2006.
- [10] PS Eriksen. *Geodesics connected with the fisher metric on the multivariate normal manifold*. Institute of Electronic Systems, Aalborg University Centre, 1986.

- [11] Minyeon Han and Frank C Park. DTI segmentation and fiber tracking using metrics on multivariate normal distributions. *Journal of mathematical imaging and vision*, 49:317–334, 2014.
- [12] Harold Hotelling. Spaces of statistical parameters. *Bull. Amer. Math. Soc*, 36:191, 1930.
- [13] Takuro Imai, Akira Takaesu, and Masato Wakayama. Remarks on geodesics for multivariate normal models. 2011.
- [14] Hiroto Inoue. Group theoretical study on geodesics for the elliptical models. In *Geometric Science of Information: Second International Conference, GSI 2015, Palaiseau, France, October 28-30, 2015, Proceedings 2*, pages 605–614. Springer, 2015.
- [15] A. T. James. The variance information manifold and the functions on it. In *Multivariate Analysis-III*, pages 157–169. Elsevier, 1973.
- [16] Peihua Li, Qilong Wang, Hui Zeng, and Lei Zhang. Local log-Euclidean multivariate Gaussian descriptor and its application to image classification. *IEEE transactions on pattern analysis and machine intelligence*, 39(4):803–817, 2016.
- [17] Tengyuan Liang, Tomaso Poggio, Alexander Rakhlin, and James Stokes. Fisher-Rao metric, geometry, and complexity of neural networks. In *The 22nd international conference on artificial intelligence and statistics*, pages 888–896. PMLR, 2019.
- [18] Maher Moakher and Mourad Zéraï. The Riemannian geometry of the space of positive-definite matrices and its application to the regularization of positive-definite matrix-valued data. *Journal of Mathematical Imaging and Vision*, 40(2):171–187, 2011.
- [19] Frank Nielsen. Cramér-Rao lower bound and information geometry. *Connected at Infinity II: A Selection of Mathematics by Indians*, pages 18–37, 2013.
- [20] Frank Nielsen. On the Jensen–Shannon symmetrization of distances relying on abstract means. *Entropy*, 21(5):485, 2019.
- [21] Frank Nielsen. The Siegel–Klein Disk: Hilbert Geometry of the Siegel Disk Domain. *Entropy*, 22(9):1019, 2020.
- [22] Richard Nock and Frank Nielsen. Fitting the smallest enclosing Bregman ball. In *Machine Learning: ECML 2005: 16th European Conference on Machine Learning, Porto, Portugal, October 3-7, 2005. Proceedings 16*, pages 649–656. Springer, 2005.
- [23] Atsumi Ohara. Doubly autoparallel structure on positive definite matrices and its applications. In *International Conference on Geometric Science of Information*, pages 251–260. Springer, 2019.
- [24] Marine Picot, Francisco Messina, Malik Boudiaf, Fabrice Labeau, Ismail Ben Ayed, and Pablo Piantanida. Adversarial robustness via Fisher-Rao regularization. *IEEE Transactions on Pattern Analysis and Machine Intelligence*, 2022.
- [25] Marion Pilté and Frédéric Barbaresco. Tracking quality monitoring based on information geometry and geodesic shooting. In *2016 17th International Radar Symposium (IRS)*, pages 1–6. IEEE, 2016.

- [26] Julianna Pinele, João E Strapasson, and Sueli IR Costa. The Fisher–Rao distance between multivariate normal distributions: Special cases, bounds and applications. *Entropy*, 22(4):404, 2020.
- [27] Branislav Popović, Marko Janev, Lidija Krstanović, Nikola Simić, and Vlado Delić. Measure of Similarity between GMMs Based on Geometry-Aware Dimensionality Reduction. *Mathematics*, 11(1):175, 2022.
- [28] C Radhakrishna Rao. Information and accuracy attainable in the estimation of statistical parameters. *Bulletin of the Calcutta Mathematical Society*, 37(3):81–91, 1945.
- [29] Carl Ludwig Siegel. *Symplectic geometry*. Elsevier, 2014. first printed in 1964.
- [30] Lene Theil Skovgaard. A Riemannian geometry of the multivariate normal model. *Scandinavian journal of statistics*, pages 211–223, 1984.
- [31] João E Strapasson, Julianna PS Porto, and Sueli IR Costa. On bounds for the Fisher-Rao distance between multivariate normal distributions. In *AIP Conference Proceedings*, volume 1641, pages 313–320. American Institute of Physics, 2015.
- [32] Mengjiao Tang, Yao Rong, Jie Zhou, and X Rong Li. Information geometric approach to multisensor estimation fusion. *IEEE Transactions on Signal Processing*, 67(2):279–292, 2018.
- [33] Geert Verdoolaege. A new robust regression method based on minimization of geodesic distances on a probabilistic manifold: Application to power laws. *Entropy*, 17(7):4602–4626, 2015.
- [34] Geert Verdoolaege and Paul Scheunders. On the geometry of multivariate generalized Gaussian models. *Journal of mathematical imaging and vision*, 43:180–193, 2012.
- [35] Wen Wang, Ruiping Wang, Zhiwu Huang, Shiguang Shan, and Xilin Chen. Discriminant analysis on Riemannian manifold of Gaussian distributions for face recognition with image sets. In *Proceedings of the IEEE conference on computer vision and pattern recognition*, pages 2048–2057, 2015.
- [36] Joseph Wells, Mary Cook, Karleigh Pine, and Benjamin D Robinson. Fisher-Rao distance on the covariance cone. *arXiv preprint arXiv:2010.15861*, 2020.